ORIGINAL ARTICLE

3D PET/CT [82]Rb PET myocardial blood flow quantification: comparison of half-dose and full-dose protocols

Martin Lyngby Lassen[1] · Osamu Manabe[1,2] · Yuka Otaki[1] · Evann Eisenberg[1] · Phi T. Huynh[1] · Frances Wang[1] · Daniel S. Berman[1] · Piotr J. Slomka[1]

Abstract

Purpose Quantification of myocardial blood flow (MBF) has become central in the clinical application of Rubidium-82 ([82]Rb) PET myocardial perfusion scans. Current recommendations suggest injections of 1100–1500 MBq of [82]Rb in bolus form, which poses a potential risk of PET system saturation on most 3D PET/CT systems currently being used. We aimed to evaluate the frequency and impact of PET system saturation and to test the potential use of a half-dose acquisition protocol.

Methods This study comprised 20 patients who underwent repeated rest scans in a single imaging session, one employing a full-dose (FD), and the other scan a half-dose (HfD) protocol. Datasets were evaluated for saturation based on visual assessments of input functions and sinograms. We compared FD and HfD MBF measurements using Bland–Altman plots, coefficients of variation (CV), and paired t tests. A correction factor permitting serial analyses using FD/HfD imaging protocols was obtained using only the datasets without saturation.

Results A dose reduction of 47% was reported for the HfD protocol (FD, 1247 ± 196 MBq; HfD, 662 ± 115 MBq). Saturation effects were observed in 4/20 (20%) FD scans, with none observed in the 20 HfD scans. Assessment of MBFs for FD and HfD protocols revealed bias in the MBF assessments of 0.09 ml/g/min (global MBF, FD = 1.03 ± 0.29 vs HfD = 0.94 ± 0.22 ml/g/min ($p = 0.001$)). Exclusion of patients with visually identified saturation effects ($N = 4$) reduced the bias to 0.05 ml/g/min (global MBF, FD = 0.97 ± 0.28 vs HfD = 0.92 ± 0.23 ml/g/min ($p = 0.02$)). From the datasets without saturation effect, it was possible to generate a bias-correction: Corrected $MBF_{HfD} = 1.09 * MBF_{HfD} - 0.03$ ml/g/min. MBF_{FD} and MBF_{HfD} did not differ following the bias correction ($MBF_{FD} = 0.97 \pm 0.28$, $MBF_{HfD,corrected} = 0.98 \pm 0.25$ ml/g/min, $p = 0.77$).

Conclusion Saturation effects can be problematic in [82]Rb MBF studies using the recommended FD protocols for 3D PET/CT scanners. The use of HfD protocol eliminates the risks of saturation and should be used instead of clinical protocols to avoid erroneous results.

Keywords Myocardial blood flow · Positron emission tomography · Rubidium · Low dose

Abbreviations
AIF   arterial input function

This article is part of the Topical Collection on Cardiology.

Electronic supplementary material The online version of this article (https://doi.org/10.1007/s00259-020-04811-0) contains supplementary material, which is available to authorized users.

✉ Piotr J. Slomka
  piotr.slomka@cshs.org

[1] Department of Imaging and Medicine, Cedars-Sinai Medical Center, Los Angeles, CA, USA

[2] Department of Nuclear Medicine, Hokkaido University of Graduate School of Medicine, Sapporo, Japan

CV	coefficient of variation
FD	full-dose
HfD	half-dose
MBF	myocardial blood flow
PET	positron emission tomography
[82]Rb	Rubidium-82

Introduction

Myocardial blood flow (MBF) measurements obtained using positron emission tomography (PET) have been documented to add prognostic value over the assessment of regional perfusion defects [1–4] and have recently been

shown to predict benefit from revascularization [5]. ^{82}Rb is the most widely used PET perfusion tracer as the tracer permits myocardial perfusion imaging in centers without a cyclotron [6–8]. Three recent joint statements from North America (ASNC and SNMMI Cardiovascular Council [1, 8]) and Europe (EANM and ESC [9]) suggest injections of 1100–1500 MBq ^{82}Rb for cardiac PET. The recommendations on injection doses were based on experiences obtained for the 2D-PET systems, where the use of physical septa's significantly reduced the scatter and limited the prompt-gamma effect [10, 11]. Injection of high doses of ^{82}Rb, however, poses a risk of saturation for 3D PET systems during the bolus injection, where highly concentrated tracer activities might be observed locally with consequential increased scatter and deadtime in the PET crystals [12, 13]. The increased deadtime in the crystals translates into apparently reduced activity distributions in the PET sinograms [14] and, thus, reduced arterial input activities observed in the input functions as a consequence [14]. The changes in the arterial input functions affect the area under the input function curve and consequently leads to incorrect MBF estimations. The frequency and effects introduced by saturation of the PET system following high dose injections of ^{82}Rb and its impact on the quantification of MBF are not yet well established.

The aims of this study were to evaluate the frequency and relative impact of saturation of 3D PET systems using a full-dose (FD) and half-dose (HfD) imaging protocol and to evaluate the differences due to using a HfD protocol versus FD for clinical assessment of MBF.

Methods

Study subjects

Twenty patients between the ages of 45 and 75 years old (11 male) underwent clinically indicated ^{82}Rb PET/CT myocardial perfusion imaging. All patients were recruited between February and August 2016, thereby covering different timepoints in the generator lifespan. The scans were acquired using current recommendations provided by the North American [1, 8] and European societies [9], respectively; employing target doses of 1500 MBq or equivalent to the delivery capabilities of the dose-cart for the FD scans, while the HfD scans targeted injections of 750 MBq. The inclusion criteria were patients aged ≥ 50 and ≤ 75 and no known cardiac disease, while exclusion criteria included known pregnancies and contraindications to ^{82}Rb. This study was performed in line with the principles of the Declaration of Helsinki. Approval was granted by the Cedars-Sinai Medical Center Institutional Review Board and written informed consent was obtained from all patients.

Full-dose and half-dose ^{82}Rb PET/CT imaging protocol

Heart rate and blood pressure were recorded before the initial ^{82}Rb injection in resting state. All datasets were acquired using the Bracco dose cart, with target deliveries of 1500 MBq (FD) and 750 MBq (HfD) in bolus form. PET imaging was performed using a whole-body 3D PET/CT scanner (Siemens Biograph-64 TruePoint PET/CT with the True V) [15]. For attenuation correction purposes, a low-dose helical CT (100 kV, pitch 1.5, 11 mAs, duration 3.4 s) was acquired in end-expiration breath-hold before each rest ^{82}Rb PET acquisition. Alignment of PET emission data and the CT attenuation correction maps were confirmed before PET-image reconstruction and corrected when necessary by the imaging technologist [15]. Figure 1 shows the imaging protocol, which consisted of two ^{82}Rb PET scans (6 min) acquired in the list-mode format. Data from both acquisitions were reconstructed into dynamic image-series consisting of 16 frames (12×10 s, 2×30 s, 1×60 s, and 1×120 s) using the vendor iterative method (Fourier rebinning + 2-dimensional attenuation-weighted ordered-subsets expectation-maximization) with 2 iterations, 8 subsets, and an 8-mm Gaussian postprocessing filter [16].

Motion correction

All reconstructed dynamic datasets were evaluated using motion correction, given the growing evidence that this is necessary to ensure high reproducibility for both rest and stress scans [17, 18]. In the current study, we applied motion correction as previously described [18], relying on manual adjustments (rigid translations) of the myocardium relative to the contour derived from the last 2-min frame. Motion correction was performed on all dynamic frames where realignment of the myocardial segmentations was judged to be necessary. Frames with identified shifts were corrected using rigid translations. All corrections were performed by an experienced nuclear medicine specialist (OM).

Quantification of MBF

Analyses of global and regional MBF assessments were obtained from the two dynamic rest imaging series—full-dose (FD) and half-dose (HfD)—with the dedicated software (QPET, Cedars-Sinai Medical Center, Los Angeles, California) [16, 19] using transaxial PET images.

MBF measurements used a standard single tissue-compartment model, as described by Lortie et al. [6], employing input functions extracted from a 2-cm^3 volume of interest located in the left ventricular lumen at the center of the mitral valve plane [20]. The global myocardium (global) as well as regional assessments for the left anterior descending (LAD), left circumflex (LCX), and right coronary artery (RCA) were reported.
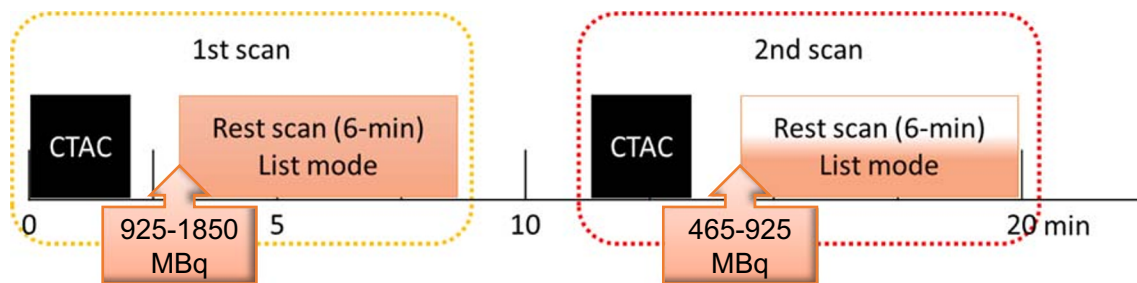
Fig. 1 Study protocol. Myocardial blood flow [82]Rb PET acquired with a full-dose and half-dose injection were compared. CT attenuation correction scans (CTAC) were obtained before each PET scan

Evaluation of PET system saturation

Saturation effects were evaluated visually from the input functions obtained in the left ventricle and sinogram data by two experienced readers. PET system saturation effects were suspected upon identification of plateau-like peaks occurring at the first-pass of the tracer-bolus (Fig. 2). Scans displaying these input-function features underwent further evaluation of the general image quality of the dynamic frames under suspicion of saturation. Identification of increased noise (speckle) (Fig. 2A and B), led to the evaluation of single slice rebinned sinograms (compressed 3D-sinograms) [21]. Saturation was declared after visually detecting changes in the count rates (obtained in the central slices of the single-slice rebinned sinogram), corresponding to the location of the myocardium (Fig. 2A) and only when a consensus was obtained by two experienced readers (ML and OM).

Reproducibility

Test–retest reproducibility of the MBF assessments was compared using the coefficient of variation (CV) using the root mean square method [22]:

$$CV = 100 \times \sqrt{\frac{\sum\left(\frac{d}{m}\right)^2}{2n.}}$$

In the equation, d represents the difference between the two paired measurements, m the mean of the paired measurements, and n the sample size.

The data were subdivided into two analyses: one included all datasets and the other excluded datasets where saturation was identified in either rest scans (FD or HfD, respectively).

Half-dose to full-dose correction

To provide a method for serial comparison of MBF$_{FD}$ and MBF$_{HfD}$ values a bias correction was obtained using datasets without saturation effects.

Statistical analysis

Continuous variables are presented as mean and standard deviations. Categorical variables are presented as absolute numbers with percentages. The correlation between MBF values was shown as correlation plots with Pearson's R correlation coefficients and Bland–Altman plots [23]. A comparison of average MBF values was tested using a paired t test. Evaluations of the within protocol (FD/HfD) variances were validated using Pitman–Morgan analyses. p values < 0.05 were considered statistically significant. Statistical calculations were carried out using MedCalc (Version 19.0.7).

Results

Global and regional MBF from the two rest acquisitions were successfully processed for all 20 patients and 60 vessels. The clinical characteristics of the study population are shown in Table 1.

Comparison between MBF-FD and MBF-HfD

Injected doses of [82]Rb were 1247 ± 196 MBq and 662 ± 115 MBq for FD and HfD acquisitions, respectively, resulting in an average 47% dose reduction for the HfD scans (Supplementary Fig. 1). Of note, the bodyweight-corrected dose was equivalent to 14.2 ± 2.4 MBq/kg and 7.5 ± 1.2 MBq/kg for the FD and HfD scans, respectively. To establish accurate MBF estimates, motion correction was applied to one of the scans (N = 7, of which 5 had corrections for FD) or both scans (N = 13). Evaluation of the MBF obtained from the FD (MBF$_{FD}$) and HfD (MBF$_{HfD}$) protocols revealed a bias of 0.09 ml/g/min for the two imaging protocols (global MBF$_{FD}$ = 1.03 ± 0.29, global MBF$_{HfD}$ = 0.94 ± 0.22, p = 0.003) (Table 2). Evaluations of the within-group variances between the FD and HfD protocols revealed significantly increased variation for both global and regional MBF assessments using the FD protocol (Pitman–Morgan analyses, Table 2). Strong correlations (Pearson's R) (≥ 0.88) were
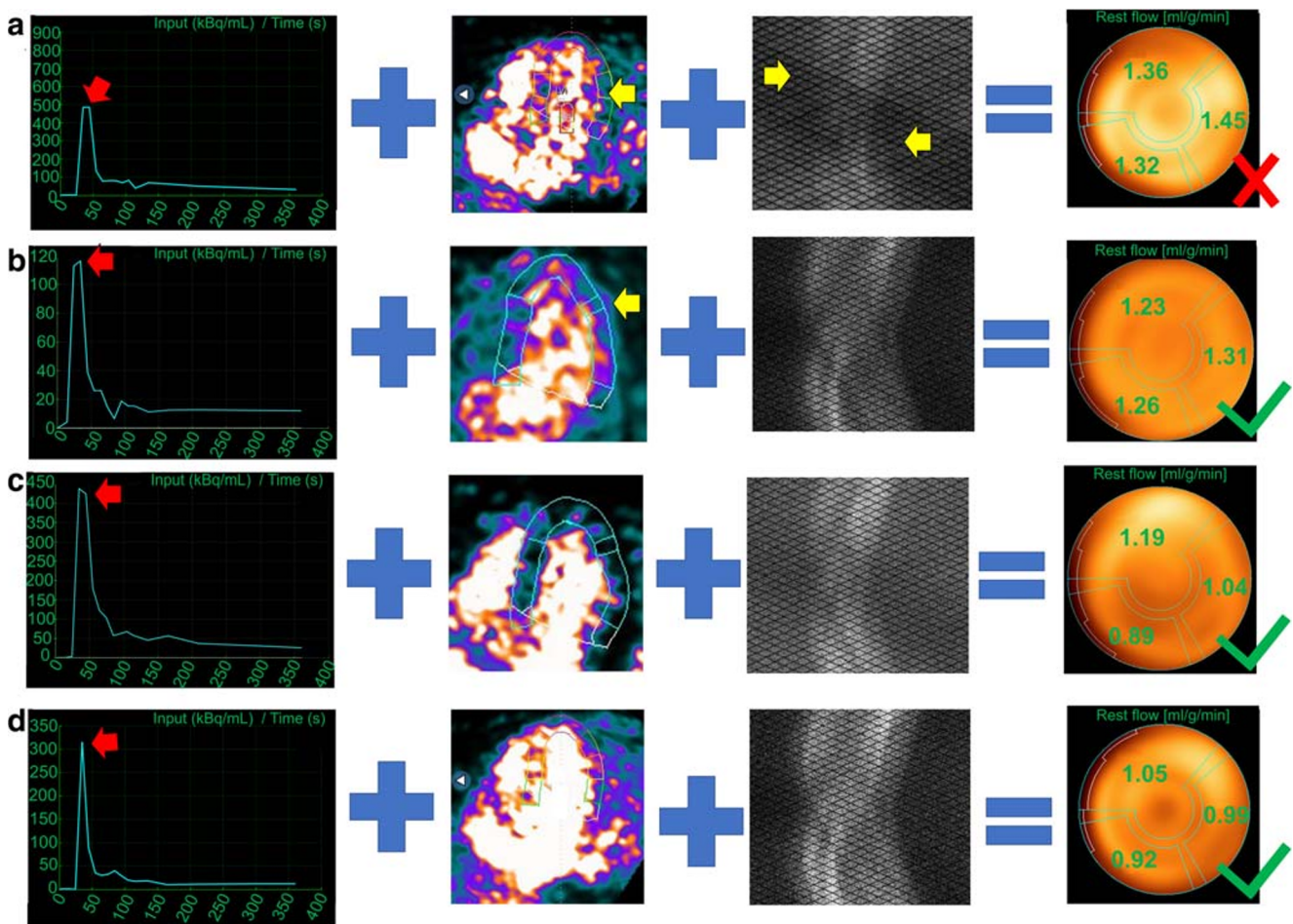
Fig. 2 Identification of PET system saturation. Identification of plateau of the aortic input function during the first-pass bolus initiated further inspections of the data. Four different cases are presented (A, B, C, D, one with PET system saturation (A), 2 where PET system saturation was suspected but ruled out through evaluations of PET images and sinograms (B and C) and finally a scan without any indication of saturation which serves a reference (D). Speckle noise in the reconstructions suggests potential saturation of the PET system (A, B), while homogenous uptake is common for non-saturated datasets. Evaluations of single-slice rebinned sinograms (3D compressed sinograms) were initiated upon identification of both: plateau findings for the input function, and increased speckle noise. PET system saturation was declared upon visually reduced uptake patterns in the sinograms (A), while normal sinogram uptake patterns excluded the saturation of the PET system (B). Case B suggests issues with count statistics for image reconstruction, while case C suggests that the first-pass arrival of the bolus happens in between two consecutive frames. For reference, case D shows an acquisition at the first-pass of the bolus (input function peak) with no signs of PET system saturation. Red x indicates PET systems saturation, whereas green checkmarks indicate images without PET system saturation

reported between the MBF_{FD} and MBF_{HfD} measurements for global and regional assessments (Table 2).

Saturation effect

A total of 4 (20%) FD scans compared to 0 (0%) HfD scans were found to be affected by PET system saturation effects. The patients in which PET system saturation was identified had ^{82}Rb injections of 1006, 1099, 1217, and 1491 MBq, respectively, thus, within the current joint statement guidelines [1, 8, 9]. The weight of the four patients were 80, 107, 92, and 107 kg with corresponding body mass indexes (BMI) of 25.8, 35.7, 30.7, and 36.8, respectively. The bodyweight-corrected doses for the 4 saturated scans were 12.7, 10.3, 13.3, and 14.0 MBq/kg and, thus, below the average weight–corrected dose observed for the FD protocol. Two case examples of saturation effects in the FD scans are shown in Fig. 3 and Supplementary Fig. 2, respectively. For all 4 patients showing signs of saturation effects, the MBF obtained using the FD protocol was increased when compared with the MBF obtained for the HfD protocol (22% difference, $MBF_{FD} = 1.25 \pm 0.22$, $MBF_{HfD} = 1.02 \pm 0.18$, $p = 0.001$). In comparison, the bias observed for the FD and HfD protocols was remarkably lower for the remaining 16 patients not showing evidence of PET system saturation, though still significantly different (5% difference, $MBF_{FD} = 0.97 \pm 0.28$, $MBF_{HfD} = 0.92 \pm 0.24$, $p = 0.019$).

Table 1 Participant Characteristics

Characteristics	Patients ($n = 20$)
Age (years old)	65 ± 9 (47–77)
Sex (male)	11 (55.0%)
BMI (kg/m^2)	31.0 ± 5.6 (19.8–37.9)
HR (beat/min)	67 ± 7 (55–77)
SBP (mmHg)	133 ± 23 (102–201)
DBP (mmHg)	70 ± 10 (51–87)
RPP (beat/min × mmHg)	9242 ± 1926 (5930–12733)
Hypertension	17 (85%)
Diabetes mellitus	6 (30%)
Dyslipidemia	12 (60%)
Smoking	2 (10%)
Family history of CAD	6 (30%)

Continuous variables are reported as mean ± SD; categorical variables are reported as n(%)

Although PET system saturation effects were identified in 4 patients, there was no correlation between injected dose and MBF (Supplementary Fig. 3).

Following the exclusion of patients with evidence of PET system saturation, there were excellent correlations between MBF obtained from FD and HfD protocols, with Pearson's $R \geq 0.93$ (Table 3). The removal of the saturated datasets ensured the harmonization of the MBF assessments in the LAD and LCX regions (Table 3, paired t test). In addition, harmonization of the within-group variation (variances observed for MBF assessments using the FD/HfD protocols) were observed for LCX and RCA (Pitman–Morgan analyses, Table 3). Despite a general harmonization in MBF assessments, some differences were observed for global measurements and in the LAD territory (Table 3).

Half-dose to full-dose serial scan correction

A bias between the full-dose MBF (MBF$_{FD}$) and the half-dose MBF (MBF$_{HfD}$) assessments was observed. From the MBF assessments obtained using the two protocols, the following linear correction of the data was obtained:

Corrected MBF$_{HfD}$: $1.09 * \text{MBF}_{HfD} - 0.03$

Reproducibility

Bland–Altman plots of global and regional MBF revealed good agreement between the MBF for the FD and the HfD imaging protocols following the exclusion of 4 saturated datasets (Fig. 4). Relative reductions in a bias of up to 37.5% were observed between the MBF$_{FD}$ and MBF$_{HfD}$ following removal of patients showing signs of PET system saturation (Bias all datasets; global = − 0.08 ml/g/min, regional − 0.09 ml/g/min; bias non-saturated datasets only; global = − 0.05 ml/g/min, regional = − 0.07 ml/g/min) (Fig. 4). Removal of the saturated datasets led to minor improvements in the test–retest reproducibility, which were found excellent for all datasets with coefficient of variation (CV) ≤ 10.4% (Table 3, Fig. 4).

Comparison of HfD/FD MBF assessments following bias correction (serial scan correction)

Applying the linear correction (Corrected MBF$_{HfD}$: $1.09 * \text{MBF}_{HfD} - 0.03$) to the MBF$_{HfD}$ assessments, harmonized both global and regional flows to the ones obtained using the FD imaging protocol (Global MBF; MBF$_{FD}$ = 0.97 ± 0.28, MBF$_{HfD}$ = 0.92 ± 0.23 (paired t test $p = 0.02$), corrected MBF$_{HfD}$: 0.98 ± 0.25, (paired t test: $p = 0.77$)) (Table 4). Additionally, no significant differences were observed for variance in the respective regional MBF values obtained from FD and HfD protocols (all p values ≥ 0.17, Pitman–Morgan analyses) (Table 4). Furthermore, test–retest variability following corrections (CV: global = 6.4%, regional (combined) = 9.1%, LAD = 11.5%, LCX = 7.7%, RCA = 7.4%, all $p \geq$ 0.46) were reported concordant with the non-corrected datasets (Table 3).

Table 2 MBFs obtained from full-dose and half-dose scans without removal of saturated datasets ($N = 20$)

	MBF$_{FD}$ (ml/g/min)	MBF$_{HfD}$ (ml/g/min)	Pearson's R	CV	Paired t test for MBF values	Pitman–Morgan test for variance of data
Global	1.03 ± 0.29	0.94 ± 0.22	0.95	8.3	**$p = 0.003$**	**$p = 0.003$**
Regional (average)	1.03 ± 0.29	0.94 ± 0.23	0.91	13.1	**$p < 0.001$**	**$p < 0.001$**
LAD	1.02 ± 0.31	0.93 ± 0.23	0.88	10.4	**$p = 0.023$**	**$p = 0.010$**
LCX	1.06 ± 0.30	0.98 ± 0.23	0.92	9.0	**$p = 0.012$**	**$p = 0.005$**
RCA	1.00 ± 0.27	0.91 ± 0.24	0.93	9.4	**$p < 0.001$**	$p = 0.235$

Continuous variables reported as mean ± SD. $p < 0.05$ values are shown in bold. *MBF*, myocardial blood flow; *LAD*, left anterior descending artery; *LCX*, left circumflex artery; *RCA*, right coronary artery; *CV*, coefficient of variation; *MBF$_{FD}$*, MBF obtained from FD scan; *MBF$_{HfD}$*, MBF obtained from HfD scan
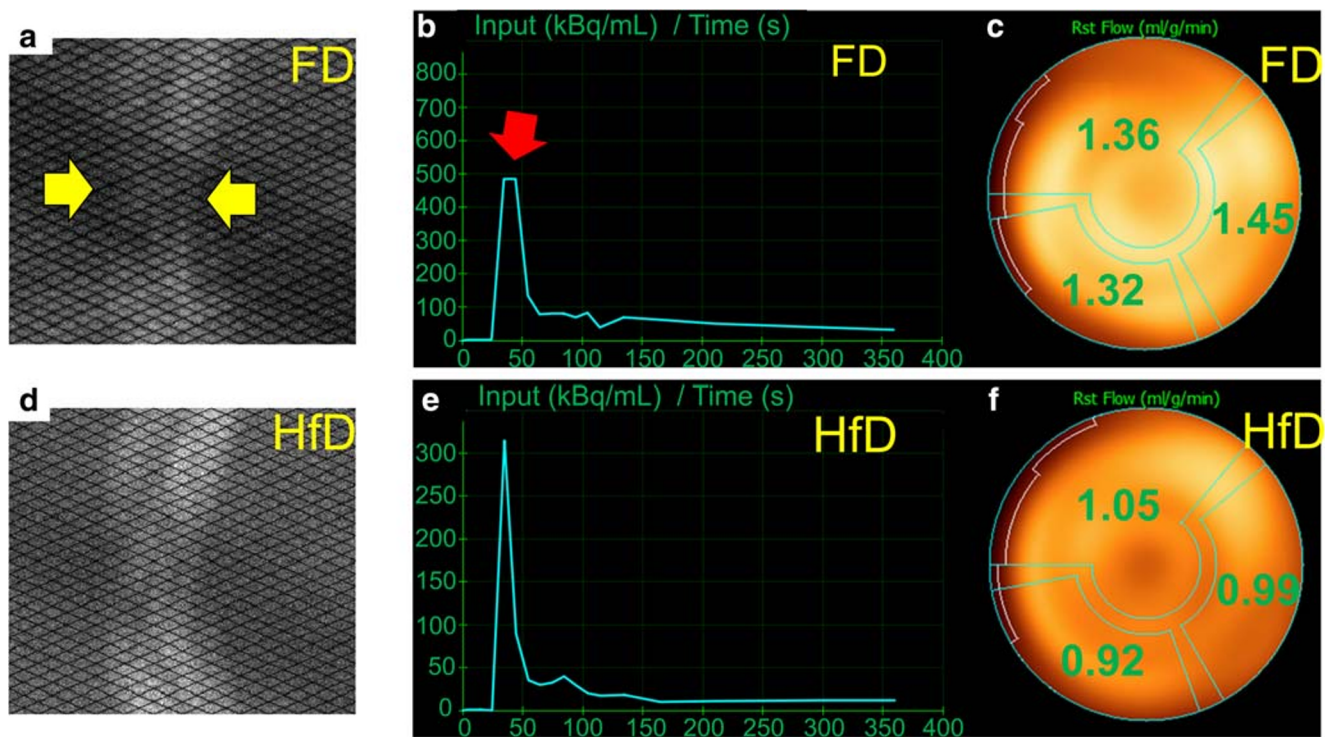
Fig. 3 Case example from our study for a 70-year-old female. Sinograms (A, D), dynamic curves of input function (B, E) and polar maps (C, F) derived from the full-dose (FD) and half-dose (HfD) injection are displayed. Compressed sinograms (summed in the axial direction) present the count profiles for a 5 s duration at the time of the peak (B, E). Sinogram representation for FD scan shows reduced counts in the center part indicating saturation of the scanner (A; yellow arrows). On the contrary, the HfD scan does not have the same saturation effect in the central part of the sinogram (D). For the FD injection, the dynamic curve shows the sign of the plateau (B; red arrow) which increases the MBF for the FD scan with more than 0.3 ml/g/min compared to the HfD scan (C, F)

Discussion

This study evaluated the frequency and impact of PET system saturation using the current clinical guidelines for ^{82}Rb MBF evaluations with 3D PET systems [1, 8], as well as the potential use of a half-dose imaging protocol. The main finding of this study was a relatively high frequency of saturation in PET systems when using the current guideline proposed injection doses (20% of the scans), which was reduced to 0% when halving the injected dose. The significant differences observed

for the MBF assessments using the FD and HfD protocol are likely due to generally increased crystal deadtimes observed for the FD acquisitions.

In the current study, three important observations were noted following dose reduction. First, the saturation of the PET system led to a systematic increase in the MBF values for the affected scans, resulting in an increased discrepancy of the MBF_{FD} and MBF_{HfD} when compared with patients without saturation effects. Secondly, MBF_{FD} and MBF_{HfD} obtained for datasets without saturation effects demonstrated high

Table 3 MBF_{FD} and MBF_{HfD} using only datasets without saturation for the full-dose scans ($N = 16$)

	MBF_{FD} (ml/g/min)	MBF_{HfD} (ml/g/min)	Pearson's R	CV	Paired t test for MBF values	Pitman–Morgan test for variance of data
Global	0.97 ± 0.28	0.92 ± 0.23	0.97	6.0	**$p = 0.019$**	**$p = 0.012$**
Regional (average)	0.97 ± 0.28	0.92 ± 0.24	0.93	9.0	**$p = 0.002$**	**$p = 0.002$**
LAD	0.96 ± 0.31	0.92 ± 0.23	0.93	10.4	$p = 0.233$	**$p = 0.013$**
LCX	1.01 ± 0.29	0.97 ± 0.24	0.94	7.2	$p = 0.118$	$p = 0.087$
RCA	0.96 ± 0.25	0.88 ± 0.25	0.95	9.0	**$p = 0.002$**	$p = 0.955$

Continuous variables reported as mean ± SD. $p < 0.05$ values are shown in bold. *MBF*, myocardial blood flow; *LAD*, left anterior descending artery; *LCX*, left circumflex artery; *RCA*, right coronary artery; *CV*, coefficient of variation; *MBF_FD*, MBF obtained from FD scan; *MBF_HfD*, MBF obtained from HfD scan
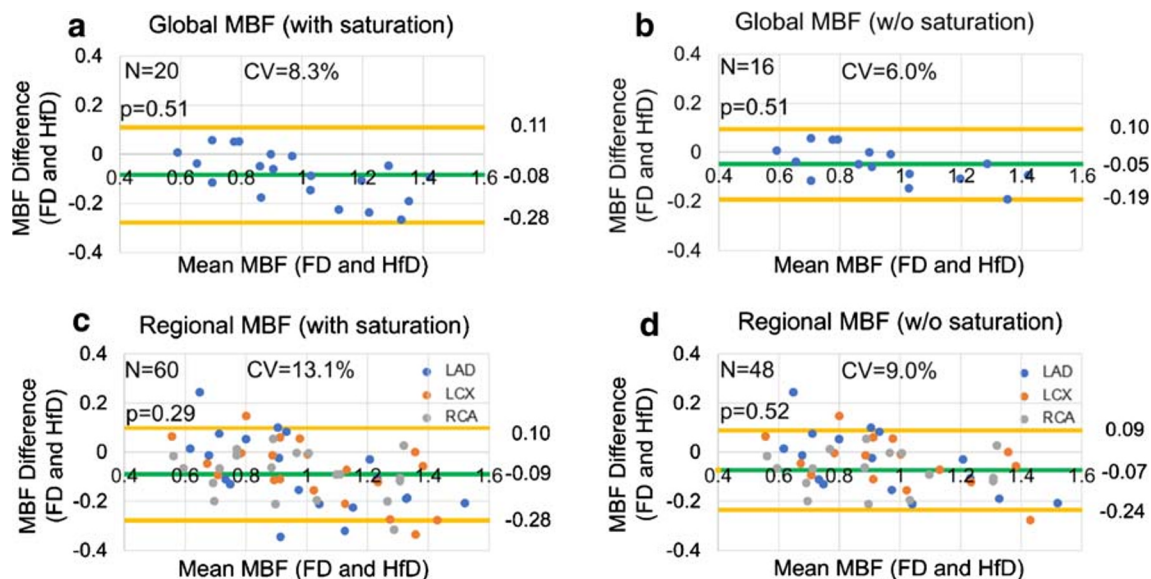
Fig. 4 Bland–Altman plots of global and regional MBF before and after the exclusion of saturated datasets. Reduced variations are observed following the removal of the saturated datasets. Mean differences are represented with the green line, while the yellow lines mark the 95% confidence limits. MBF, myocardial blood flow [ml/g/min], w/o = without; FD, full-dose; HfD, half-dose; CV, coefficient of variation

linearity with Pearson's $R \geq 0.93$, although bias was observed for the two protocols. The third observation was high test–retest repeatability measures with no statistical differences of either MBFs obtained for the FD and HfD protocols following a simple linear correction (test for MBF measurements: all $p \geq 0.77$ (paired t test), variances (per territory and global MBF assessments for the FD and HfD protocols, respectively) all $p \geq 0.17$ (Pitman–Morgan test).

The FD acquisition protocol was based on the most recent joint positions in North America (between ASNC and SNMMI Cardiovascular Council [1, 8]) and in Europe (between EANM and ESC [9]), which both suggest target doses of 1100–1500 MBq when using lutetium orthosilicate injected (LSO) 3D PET systems. These recommendations for relatively high doses of ^{82}Rb are in part due to the technical

drawbacks of ^{82}Rb (short half-life and a low extraction fraction), while still facilitate reliable MBF measurements [24]. Although these recommendations are proposed for the 3D systems, the use of high-dose injections arose from the 2D PET systems, where increased doses were necessary to obtain sufficient image-quality. The high-dose protocols were originally required because of the use of physical septa, which significantly reduced the sensitivity of the systems when compared with the modern 3D systems [12, 25]. The increased sensitivity of the modern 3D PET systems, however, increases the risks of saturating when high tracer-activities are injected in bolus-forms such as in ^{82}Rb scans [13, 14].

To avoid the risk of PET system saturation, alternative protocols using a slow-infusion of the tracer activity over 30 s have been proposed [26–28]. Unfortunately, the use of the

Table 4 MBF assessments before and after bias correction of MBF$_{HfD}$ data

	MBF values (ml/g/min)	Paired t test for MBF values	Pitman–Morgan test for variance of data
Global MBF assessments			
MBF$_{FD}$	0.97 ± 0.28	N/A	N/A
MBF$_{HfD}$	0.92 ± 0.23	$\boldsymbol{p = 0.02}$	$\boldsymbol{p = 0.01}$
corrected MBF$_{HfD}$	0.98 ± 0.25	$p = 0.77$	$p = 0.17$
Regional MBF assessments (combined)			
MBF$_{FD}$	0.97 ± 0.28	N/A	N/A
MBF$_{HfD}$	0.92 ± 0.24	$\boldsymbol{p < 0.01}$	$\boldsymbol{p < 0.01}$
corrected MBF$_{HfD}$	0.98 ± 0.26	$p = 0.84$	$p = 0.27$

Continuous variables reported as mean $\pm$ SD. $p < 0.05$ values are shown in bold. *MBF*, myocardial blood flow; *CV*, coefficient of variation; *MBF$_{FD}$*, MBF obtained from FD scan; *MBF$_{HfD}$*, MBF obtained from HfD scan

slow-infusion protocols is not possible in the commercial products, where the commercial dose-carts target a constant flow through the generator, with tracer administration in bolus form as a consequence [26]. Another approach, focusing more on optimizing the image-quality, proposed to employ weight-specific injection profiles for a range of different PET systems [12]. The study showed the feasibility of employing patient-weight specific injection profiles, thus, avoiding saturation effects of the PET system. However, using such protocols increase the time spent on scan preparations for each scan where the dose-delivery cart needs calibration between the PET system and delivery carts. This can introduce nonconformities of the dose-deliveries with a bias of up to 68% being reported [12]. In a study by Tout et al. [14], the authors recommended using injection-profiles (bolus-injection) of 1110 MBq for the assessments of MBF to avoid PET system saturation. Although this injection profile might reduce the risks of PET system saturation, two of the four scans in the current study where PET system saturation was reported had injected doses of 1006 and 1099 MBq and, thus, below the recommended 1110 MBq injection profiles.

In the current study, we focused on the potential use of a fixed dose across all patients (HfD scan protocol) and its impact on MBF evaluations. Using the HfD protocol, no dependencies between injected activities and MBF estimates were observed (Supplementary Fig. 3). Furthermore, the test–retest repeatability measures obtained for the FD and HfD protocols were comparable to a recent study evaluating short-term reproducibility of MBF obtained using an FD/FD protocol from our center [18]). A general bias between the FD and HfD protocol for the MBF_{FD} and MBF_{HfD} was observed (0.05 ml/g/min), suggesting a small reduction for the MBF_{HfD} evaluations with lower dose. Of note, while the 0.05 ml/g/min bias in the test–retest study appears somewhat increased in comparison to a recent study from our center evaluating short-term test–retest reproducibility using an FD protocol (0.02 ml/g/min bias) [18], both biases are not significantly > 0. This is potentially due to the relatively small sample in both studies (20 patients in the current cohort and 21 patients in our FD/FD test–retest reproducibility study [18]). However, it is also possible that these differences are due to the normal variability within one patient. Nevertheless, to facilitate serial comparisons between MBF evaluations obtained using the HfD and the standard HD protocols, we developed a bias correction factor compensating for the general reduction in MBF observed for HfD protocol. The correction factor was established using only datasets without any visible saturation effects to exclude potential bias in the corrections from the saturated data. Following the corrections, no significant differences between the MBF_{FD} and corrected MBF_{HfD} were observed. Based on these findings, no detectable differences

in the bias for the two studies, and the FD scan to HfD repeatability coefficient being comparable with FD/FD scan–rescan repeatability [18], we propose the use of HfD protocol instead of the FD protocols for MBF evaluations to minimize the risks of PET system saturation.

One limitation of this study is the saturation effect was not evaluated during the stress scan. It was not possible to perform a second stress scan in the same imaging session with repeated pharmacological stress agent injection within this time. Additionally, the physiological variations due to the different stress responses would be large and potentially biased during repeated stress scan. Nevertheless, the injected doses are similar at stress and rest so similar saturation effects could be expected. Our study has several additional limitations. The limitation of the proposed HfD to FD correction technique is that it was tested and validated within the same cohort. A prospective trial will be required to fully validate this technique. Another limitation is the number of participants evaluated in this study, which is relatively small, rendering it difficult to determine whether the small bias between FD and HfD MBF estimates being caused by a potential type 2 error or by differences in the count-rates caused by the differences in the two injection profiles. However, despite the sample size, a significant correlation between the MBF_{HfD} and MBF_{FD} was identified. Another limitation of the study was that blood pressure and heart rate was only obtained before the initial scan (FD) such that MBF estimates cannot be corrected for changes in the RPP. The PET/CT system used for the clinical evaluations were based on older technology. The use of solid-state PET systems might reduce the frequency and risk of saturation because of the generally reduced dead-time and reduced bias in the detected activities [29]. However, most current PET systems still rely on photomultiplier tube technology where saturation effects still pose a risk of PET system saturation, with frequencies similar to the ones presented in the current study [14]. Finally, a limiting factor of this study is that all saturation effects were evaluated retrospectively using sinograms, without the access to the saturation profiles of the individual detectors. We also did not study the quality of static or gated perfusion images; the quality of static perfusion image, however, is not affected by saturation due to the fast decay of the tracer and distribution in the body [30]. Nevertheless, HfD static or gated perfusion images are created from the same PET acquisition and may potentially suffer from increased noise. The effect of dose reduction on static and gated perfusion images will need to be separately evaluated in comparison to full-dose studies before half-dose ^{82}Rb are deployed clinically; however, these effects could be evaluated retrospectively from list-mode data in larger populations with external reference standards.

Conclusions

In this study, we report that up to 20% (4 of 20 scans) of all rest ^{82}Rb cardiac PET scans with injected doses of 925–1480 MBq suffered from saturation effects in the first-generation 3D PET/CT systems; whereas repeated acquisitions using a dose of 480–900 MBq in the same patients did not result in saturation.

Compliance with ethical standards

Conflict of interests The authors declare that they have no conflict of interest.

Ethical approval and informed consent All procedures performed in studies involving human participants were in accordance with the ethical standards of the institutional and/or national research committee and with the 1964 Helsinki declaration and its later amendments or comparable ethical standards. Approval for this study was granted by the Cedars-Sinai Medical Center Institutional Review Board and written informed consent was obtained from all patients.

References

1. Murthy VL, Bateman TM, Beanlands RS, Berman DS, Borges-Neto S, Chareonthaitawee P, et al. Clinical quantification of myocardial blood flow using PET: joint position paper of the SNMMI cardiovascular council and the ASNC. J Nucl med [internet]. Springer US; 2018;59:273–93. Available from: https://doi.org/10.1007/s12350-017-1110-x.

2. Farhad H, Dunet V, Bachelard K, Allenbach G, Kaufmann PA, Prior JO. Added prognostic value of myocardial blood flow quantitation in rubidium-82 positron emission tomography imaging. Eur Heart J Cardiovasc Imaging. 2013;14:1203–10.

3. Murthy VL, Naya M, Foster CR, Hainer J, Gaber M, Di Carli G, et al. Improved cardiac risk assessment with noninvasive measures of coronary flow reserve. Circulation Am Heart Assoc. 2011;124:2215–24.

4. Ziadi MC, deKemp RA, Williams KA, Guo A, Chow BJW, Renaud JM, et al. Impaired myocardial flow reserve on rubidium-82 positron emission tomography imaging predicts adverse outcomes in patients assessed for myocardial ischemia. J Am Coll Cardiol. 2011;58:740–8.

5. Patel KK, Spertus JA, Chan PS, Sperry BW, Al Badarin F, Kennedy KF, et al. Myocardial blood flow reserve assessed by positron emission tomography myocardial perfusion imaging identifies patients with a survival benefit from early revascularization 2019;1–11.

6. Lortie M, Beanlands RSB, Yoshinaga K, Klein R, DaSilva JN, DeKemp RA. Quantification of myocardial blood flow with 82Rb dynamic PET imaging. Eur J Nucl Med Mol Imaging. 2007;34:1765–74.

7. Bateman TM, Dilsizian V, Beanlands RS, DePuey EG, Heller G V, Wolinsky DA, et al. American Society of Nuclear Cardiology and Society of Nuclear Medicine and Molecular Imaging Joint position statement on the clinical indications for myocardial perfusion PET.

8. Dilsizian V, Bacharach SL, Beanlands RS, Bergmann SR, Delbeke D, Dorbala S, et al. ASNC imaging guidelines/SNMMI procedure standard for positron emission tomography (PET) nuclear cardiology procedures. J Nucl Cardiol. 2016;23:1187–226.

9. Hesse B, Tägil K, Cuocolo A, Anagnostopoulos C, Bardiés M, Bax J, et al. EANM/ESC procedural guidelines for myocardial perfusion imaging in nuclear cardiology. Eur J Nucl Med Mol Imaging. 2005;32:855–97.

10. Esteves FP, Nye JA, Khan A, Folks RD, Halkar RK, Garcia EV, et al. Prompt-gamma compensation in Rb-82 myocardial perfusion 3D PET/CT. J Nucl Cardiol. 2010;17:247–53.

11. Cherry SR, Dahlbom M, Hoffman EJ. 3D PET using a conventional multislice tomograph without septa. J Comput Assist Tomogr. 1991;15:655–68.

12. Renaud JM, Yip K, Guimond J, Trottier M, Pibarot P, Turcotte E, et al. Characterization of 3-dimensional PET Systems for Accurate Quantification of myocardial blood flow. J Nucl Med [internet]. 2017;58:103–9. Available from: **http://www.ncbi.nlm.nih.gov/pubmed/27539843**.

13. Lodge MA, Badawi RD, Gilbert R, Dibos PE, Line BR. Comparison of 2-dimensional and 3-dimensional acquisition for 18F-FDG PET oncology studies performed on an LSO-based scanner. J Nucl Med Soc Nuclear Med. 2006;47:23–31.

14. Tout D, Tonge CM, Muthu S, Arumugam P. Assessment of a protocol for routine simultaneous myocardial blood flow measurement and standard myocardial perfusion imaging with rubidium-82 on a high count rate positron emission tomography system. Nucl Med Commun. 2012;33:1202–11.

15. Slomka PJ, Diaz-Zamudio M, Dey D, Motwani M, Brodov Y, Choi D, et al. Automatic registration of misaligned CT attenuation correction maps in Rb-82 PET/CT improves detection of angiographically significant coronary artery disease. J Nucl Cardiol. 2015;22:1285–95.

16. de Kemp RA, Declerck J, Klein R, Pan X-B, Nakazato R, Tonge C, et al. Multisoftware reproducibility study of stress and rest myocardial blood flow assessed with 3D dynamic PET/CT and a 1-tissue-compartment model of 82Rb kinetics. J Nucl Med. 2013;54:571–7.

17. Armstrong IS, Memmott MJ, Saint KJ, Saillant A, Hayden C, Arumugam P. Assessment of motion correction in dynamic rubidium-82 cardiac PET with and without frame-by-frame adjustment of attenuation maps for calculation of myocardial blood flow. J Nucl Cardiol [Internet]. Springer International Publishing; 2019; **Available from:** http://link.springer.com/10.1007/s12350-019-01834-5

18. Otaki Y, Lassen ML, Manabe O, Eisenberg E, Gransar H, Wang F, et al. Short-term repeatability of myocardial blood flow using 82 Rb PET/CT: the effect of arterial input function position and motion correction. J Nucl Cardiol Springer; 2019;1–8.

19. Nakazato R, Berman DS, Dey D, Le Meunier L, Hayes SW, Fermin JS, et al. Automated quantitative Rb-82 3D PET/CT myocardial perfusion imaging: normal limits and correlation with invasive coronary angiography. J Nucl Cardiol. 2012;19:265–76.

20. Vasquez AF, Johnson NP, Gould KL. Variation in quantitative myocardial perfusion due to arterial input selection. JACC Cardiovasc Imaging [Internet]. Elsevier Inc.; 2013;6:559–68. **Available from:** https://doi.org/10.1016/j.jcmg.2012.11.015

21. Daube-Witherspoon ME, Muehllehner G. Treatment of axial data in three-dimensional PET. J Nucl Med [Internet]. 1987;28:1717–24. Available from: **http://www.ncbi.nlm.nih.gov/pubmed/3499493**.

22. Hyslop NP, White WH. Estimating precision using duplicate measurements. J Air Waste Manage Assoc. 2009;59:1032–9.

23. Klein R, Renaud JM, Ziadi MC, Thorn SL, Adler A, Beanlands RS, et al. Intra-and inter-operator repeatability of myocardial blood flow and myocardial flow reserve measurements using rubidium-82 pet

J Nucl Med [Internet]. 2016;57:1654–6. Available from: http://www.ncbi.nlm.nih.gov/pubmed/27561879.

and a highly automated analysis program. J Nucl Cardiol. 2010;17:600–16.

24. Nakazato R, Berman D, Alexanderson E, Slomka P. Myocardial perfusion imaging with PET. Imaging Med [Internet] 2013;5:35–46. **Available from:** http://www.pubmedcentral.nih.gov/articlerender.fcgi?artid=3650901&tool=pmcentrez&rendertype=abstract

25. de Kemp RA, Yoshinaga K, Beanlands RSB. Will 3-dimensional PET-CT enable the routine quantification of myocardial blood flow? J Nucl Cardiol. 2007;14:380–97.

26. Klein R, Ocneanu A, de Kemp RA. Time-frame sampling for 82Rb PET flow quantification: towards standardization of clinical protocols. J Nucl Cardiol. Springer US; 2017;24:1530–4.

27. Lautamäki R, Brown TLY, Merrill J, Bengel FM. CT-based attenuation correction in 82Rb-myocardial perfusion PET-CT: incidence of misalignment and effect on regional tracer distribution. Eur J Nucl Med Mol Imaging. 2008;35:305–10.

28. Lautamäki R, George RT, Kitagawa K, Higuchi T, Merrill J, Voicu C, et al. Rubidium-82 PET-CT for quantitative assessment of myocardial blood flow: validation in a canine model of coronary artery stenosis. Eur J Nucl Med Mol Imaging. 2009;36:576–86.

29. van Dijk JD, Jager PL, van Osch JAC, Khodaverdi M, van Dalen JA. Comparison of maximal Rubidium-82 activities for myocardial blood flow quantification between digital and conventional PET systems. J Nucl Cardiol [Internet]. Springer US; 2018;26:1–6. Available from: https://doi.org/10.1007/s12350-017-1156-9.

30. Dasari PKR, Jones JP, Casey ME, Liang Y, Dilsizian V, Smith MF. The effect of time-of-flight and point spread function modeling on 82Rb myocardial perfusion imaging of obese patients. J Nucl Cardiol [Internet]. Springer US; 2018; **Available from:** https://doi.org/10.1007/s12350-018-1311-y